

## An imaging heavy ion beam probe diagnostic for the ASDEX Upgrade tokamak

J.Galdon-Quiroga<sup>1</sup>, G.Birkenmeier<sup>1,2</sup>, V.Olevskaia<sup>1,2</sup>, M.Sochor<sup>1</sup>, G.Anda<sup>3</sup>, K.Bald<sup>1</sup>,  
M.Dunne<sup>1</sup>, M.Garcia-Munoz<sup>4</sup>, A.Herrmann<sup>1</sup>, K.Kaunert<sup>1</sup>, D.Nagy<sup>3</sup>, J.F.Rivero-Rodriguez<sup>4</sup>,  
M.Rodriguez-Ramos<sup>4</sup>, V.Rohde<sup>1</sup>, E.Strumberger<sup>1</sup>, J.J. Toledo<sup>4</sup>, E.Viezza<sup>4</sup>,  
E.Wolfrum<sup>1</sup>, S.Zoletnik<sup>3</sup>, U.Stroth<sup>1,2</sup> and the ASDEX Upgrade<sup>4</sup> Team

<sup>1</sup> Max Planck Institute for Plasma Physics, Garching, Germany

<sup>2</sup> Physics Department E28, Technical University of Munich, Garching, Germany

<sup>3</sup> Wigner RCP, EURATOM Association HAS, Budapest, Hungary

<sup>4</sup> Centro Nacional de Aceleradores (CNA), University of Seville, Spain

### **Introduction**

A new diagnostic - the imaging heavy ion beam probe (i-HIBP) [1, 2] - for the simultaneous measurement of plasma potential, magnetic field and density fluctuations is being developed at the ASDEX Upgrade (AUG) tokamak. The diagnostic uses an ion beam in order to extract information of the plasma as in classical heavy ion beam probes (HIBP) [3], but uses an injector technology similar to those of beam emission spectroscopy (BES) diagnostics and a scintillator plate as particle detector like in fast-ion loss detectors (FIELD) [4]. The measurement principle is illustrated in Fig.1 of reference [1]. A neutral beam of heavy atoms (Cs in this case) is launched into the plasma with an energy of 70 keV. As this neutral *primary* beam penetrates the plasma, it is ionized leading to the generation of a fan of charged *secondary* beams which are deflected by the tokamak magnetic field. The fan of secondary beams is collected by a scintillator plate placed behind the limiter shadow of the machine. The selected scintillator material is the so called TG-Green ( $SrGa_2S_4 : Eu^{2+}$ ), widely used in other diagnostics such as FILDs. The light pattern emitted by the scintillator, which is imaged by a fast camera, contains radially resolved information about the density, potential and magnetic field in the edge and scrape-off layer regions of the plasma. The use of a neutral primary beam allows to reduce the probing beam energy compared to standard HIBPs, while the use of an in-vessel scintillator as detection system makes the system more compact and improves the radial resolution of the system.

The plasma density can be recovered from the intensity measurement, while displacements of the light pattern - in the following strike-pattern - provide information about plasma potential and magnetic field fluctuations. Magnetic field fluctuations, such as those expected due to changes in the current density profile, lead to a shift of the whole strike-pattern, while fluctuations of the plasma potential lead to local shifts of the strike-pattern. This way the displace-

ments due to magnetic field and potential perturbations can be discriminated. The difference in the time-scales of the phenomena to be investigated can also be used for discrimination.

### ***Beam modelling***

The trajectories of the secondary beams have been calculated with the full-orbit following code FIOS [1], which can handle 3D electric and magnetic fields. It was found that the toroidal field ripple should be included in the simulations since it can lead to a shift of the strike-pattern of up to  $\sim 3.5$  cm, if an inappropriate toroidal injection position relative to the toroidal field coils is selected. In order to calculate the signal intensity at the scintillator plate, a model for the beam attenuation has been implemented which takes into account electron impact ionization and charge exchange reactions. The model is described in references [1] and [2]. It is found that the secondary ion current density reaching the scintillator strongly depends on the plasma density profile. For a scenario with a core line averaged density of  $\bar{n}_e = 2.6 \cdot 10^{19} \text{ m}^{-3}$ , a current density of the order of  $\sim \text{mA}/\text{m}^2$  is expected at the scintillator plate, while for a scenario with  $\bar{n}_e = 7.8 \cdot 10^{19} \text{ m}^{-3}$ , the current density expected at the scintillator plate is reduced to  $\sim \text{nA}/\text{m}^2$ .

A number of simulations have been carried out to obtain the optimal parameters for the beam injection and detection geometry. The optimization process aimed at achieving maximum signal level at the scintillator plate as well as maximum strike-pattern displacements due to magnetic field and potential perturbations. At the same time, the optimization process was constrained by space limitations, port availability and compatibility with currently existing diagnostics in the same sector. The final injection parameters are for a baseline scenario with a plasma current  $I_p$  and magnetic field  $B_t$  of  $I_p/B_t = 0.8\text{MA}/2.5\text{T}$  are: toroidal injection angle  $\theta_{tor} = 5^\circ$ ; poloidal injection angle  $\theta_{pol} = 0^\circ$ , injection energy  $E_0 = 70$  keV. The radial coverage of the diagnostic is expected to be from  $\rho_{pol} > 0.85$ .

The expected range of operation of the diagnostic is expected to be wide enough to cover all the possible scenarios in forward field configuration. This is illustrated in Fig.1. In order to estimate this operational range, we assume that the injection energy of the beam should be changed for different  $B_t$  in order to keep the same effective Larmor radius of the secondary beams. Therefore, the injection energy has to be scaled as  $E_b = (\frac{B}{B_0})^2 \cdot E_0$ , where the subindex 0 refers to the baseline setup. On the other hand, we assume that variations of the plasma current lead to a global displacement of the strike-line of 1 cm / 100 kA, as inferred from the simulations discussed above. The validity of this estimation has been assessed by the strike-pattern calculation at specific scenarios, indicated by the colored diamonds in Fig.1, spanning different  $B_t$  and  $I_p$  values. The beam energy was scaled accordingly as described previously. In all cases the strike-pattern was found to lay within the scintillator limits.

A sensitivity study has been carried out to determine which physics phenomena can be investigated with the i-HIBP at AUG [5]. To this end, the displacement of the strike-pattern on the scintillator plate due to magnetic field and plasma potential fluctuations has been evaluated for different phenomena such as: current density evolution during an edge localized mode (ELM) cycle, application of externally applied magnetic perturbations (MP) or geodesic acoustic modes (GAMs) among others. The expected strike-pattern displacements and sensitivity are in agreement with those described in [1], ranging from  $\sim 0.2\text{mm}$  local shifts due to potential perturbations up to  $\sim 3\text{mm}$  global shifts due to magnetic field perturbations.

#### **Hardware arrangement: out vessel**

The main out-vessel component of the diagnostic is the beam injector. The injector will be placed in sector 13 of AUG, where the injection is done through a port located slightly above the mid-plane. The injector is oriented  $5^\circ$  toroidally towards sector 14, accordingly to the baseline injection parameters found in the previous section. The injector is based on the design described in [6] and has been provided by the Wigner Institute. The main elements are: a high-voltage cage that contains the ion source, the emitter ( $\sim 70\text{kV}$ ) and extractor ( $\sim 60\text{kV}$ ) electrodes; an electron suppression ring ( $\sim -0.5\text{kV}$ ); a pair of deflection plates for beam poloidal and toroidal steering ( $\pm 0.5\text{kV}$ ), as well as for fast beam chopping (up to 250 kHz); a neutralizer chamber; and a diagnostic chamber, which contains a Faraday cup and 2 cameras for beam monitoring, and which has been re-designed to include a set of collimators to reduce the size of the beam. An additional Faraday cup can be placed between the deflection plates and the neutralizer, and a mirror can be placed between the HV box and the deflection plates for observation of the ion source.

#### **Hardware arrangement: in vessel**

The main in-vessel components of the diagnostic are an optical head and an image guide. The optical head, shown in Fig.2 contains the scintillator plate (16.9 cm height x 6 cm width) for the measurement of the secondary beams, a thermocouple to monitor the temperature of the plate, a current measurement and a lamp. The optical head is protected by a tile on the plasma facing side, which is 2.5 cm behind the shadow of the limiter surface. The optical head has an

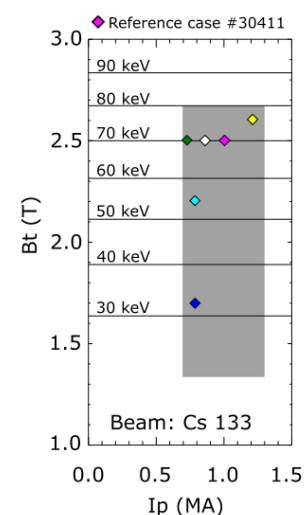


Figure 1: Estimated operational range for the i-HIBP diagnostic at AUG. The contour lines indicate the injection energy of the beam. The shaded region indicates the operational space accessible to the diagnostic, without taking into account the beam deflection plates.

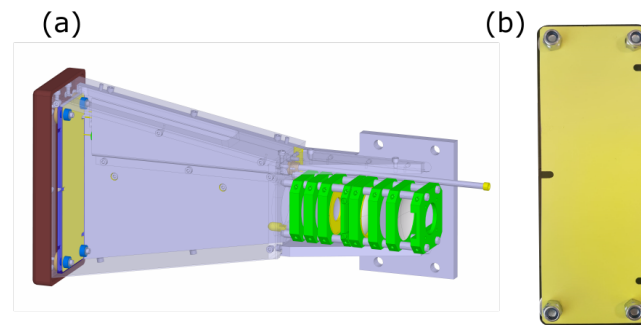


Figure 2: (a) Optical head of the i-HIBP diagnostic. (b) Picture of the scintillator powder deposited on the stainless steel plate.

opening of approximately  $\sim 5 \times 15$  cm in the top side, in order to allow the secondary beam trajectories into the scintillator. A shutter that closes this opening is also installed to avoid the coating of the scintillator during boronizations. The light emitted by the scintillator is imaged by an objective consisting of 6 lenses which projects the image of the scintillator onto a 1.8 m long SCHOTT image guide, consisting of 1700x700 glass fibers, which is then imaged from outside the vacuum window with a high speed camera.

### *Summary*

An imaging heavy ion beam probe has been designed and will be installed in the AUG tokamak. Modelling of the beam trajectories has been carried out with a full orbit following code which can handle 3D magnetic and electric fields, while the attenuation of the beam is calculated taking into account electron impact ionization and charge exchange reactions. Based on these simulations, the injection and detection geometries have been optimized while respecting the spatial restrictions, and the in- and out- vessel components have been designed accordingly. Laboratory experiments are currently ongoing to characterize the beam and the scintillator response to Cs irradiation, while the manufacturing of all components of the diagnostic is being finalized. The i-HIBP at AUG is foreseen to go in operation by the end of 2019.

### **References**

- [1] J.Galdon-Quiroga, Journal of Instr. **12**, C08023 (2017)
- [2] G.Birkenmeier et al, Journal of Instr. (submitted)
- [3] A.V. Melnikov et al, Nucl. Fusion **57**, 072004 (2017)
- [4] M.Garcia-Munoz et al, Rev. Sci. Instrum. **80**, 053503 (2009)
- [5] V.Olevskaia et al, DPG Conference (2019)
- [6] G.Anda et al, Rev. Sci. Instrum. **89**, 013503 (2018)